Stress Analysis of Silicon Membranes with Electroplated Permalloy Films Using Raman Scattering

Hyoung J. Cho, Kwang W. Oh, Chong H. Ahn, P. Boolchand, and Tae-Chul Nam

Abstract—**We have measured the stress profile on a silicon membrane electroplated with a permalloy film using Raman scattering. The effect of silicon membrane thickness and permalloy film thickness on stress distribution was studied. Depending upon the nature of stress, the optic phonon in silicon at 520 cm^{-1} either shifts upward (compressive) or downward (tensile). The phonon frequency shift is proportional to the magnitude of stress. A microscope X–Y stage was used to map the stress distribution over the silicon membrane that was covered and uncovered by the permalloy film. Silicon membranes in the thickness range, 9 μm $< t_m <$ 12 μm, and permalloy films in the thickness range, 6 μm $< t_p <$ 13 μm showed evidence of compressive stress. Based on the present results, membrane type microvalve design is optimized to prevent leakage, originating from stressed membranes. Such a nondestructive and noncontact microscopic stress analysis technique can be applied for design optimization in various magnetic MEMS devices.**

Index Terms—**MEMS, permalloy film, Raman scattering, stress analysis.**

I. Introduction

PERMALLOY thin films have been widely used for soft magnetic components in electromagnetic devices. In addition, permalloy film deposited on the silicon membrane is the most basic structure for constructing magnetic actuators and sensors [1]–[3]. However, the stress resulting from electroplated magnetic films has been one of the main factors limiting functionality of many micro magnetic devices. In general, as the size of the device decreases and the structure becomes complex, the stress from the edges and interfaces becomes more important. Thus, understanding of stress appeared on silicon membranes caused by deposited magnetic films is very essential to fabricate reliable magnetic MEMS devices. Recently, Raman spectroscopy has been recognized as a very powerful technique to measure residual stress profile in microchip devices [4]–[6]. In general, stress-induced Raman shift ($\Delta\omega$) of the 520 cm^{-1} optic phonon increases when stress is compressive and decreases when it is tensile. Compared to X-ray data, the Raman scattering reveals stress at a specific point with a spatial resolution of 1 μm [4]. However, the Raman shift is a complicated function of all the stresses and, strictly speaking, cannot be interpreted in terms of only one stress component [5]. Therefore, there have been many theoretical approaches to understand the relation between the stresses and the Raman shift [6]. In our efforts to find the optimized structure for magnetic microvalve, we have focused on the overall evaluation of stress distribution, which silicon membranes undergo, resulting from residual stress of thin silicon membrane and also from electroplated permalloy films including metallic seed layer for electroplating rather than on finding an exact expression of individual stress component.

Manuscript received October 13, 2000.

H. J. Cho, K. W. Oh, C. H. Ahn, and P. Boolchand are with the Department of Electrical and Computer Engineering and Computer Science, University of Cincinnati, Cincinnati, OH 45221-0030 USA.

T.-C. Nam is with the School of Electrical and Electronic Engineering, Yeungnam University, Kyongsan 712-749, Korea.

Publisher Item Identifier S 0018-9464(01)07165-5.

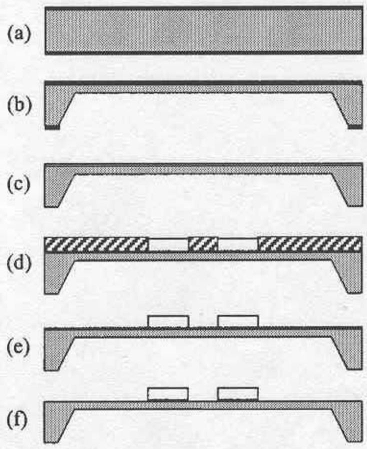

Fig. 1. Schematic illustrations of the sample fabrication: (a) oxidation of silicon wafer; (b) wet chemical etching of silicon; (c) oxide removal and metal seed layer deposition; (d) photoresist patterning and electroplating; (e) photoresist stripping and (f) metal seed layer etching.

II. Experimental

The permalloy ($Ni_{80}Fe_{20}$) films were electroplated on the silicon membranes (5 mm × 5 mm) prepared from wet chemical etching. Fig. 1 schematically describes the process for testing sample preparation. First, the silicon wafer was oxidized to obtain a 1.5 μm thick SiO_2 as a mask layer for wet chemical etching. Then, silicon membranes were made to have thickness (t_m) in the range, 9 μm $< t_m <$ 34 μm. After removing oxide, Cr (300 Å)/Cu (3000 Å) was deposited using an electron-beam evaporator as a plating seed layer. AZ-4620 photoresist was then spun on the wafer and patterned to build the electroplating mold. Electroplating was performed under the current density of 5 mA/cm^2. Table I describes the composition of a bath which has been widely used for the permalloy electroplating. Permalloy films with thickness, t_p = 6 μm and t_p = 13 μm were electroplated on the silicon membranes. After completing

TABLE I
BATH COMPOSITION FOR PERMALLOY($Ni_{80}Fe_{20}$) FILM

Chemical	Quantity(g/L water)
$NiSO_4 6H_2O$	200
$FeSO_4 7H_2O$	8
$NiCl_2 6H_2O$	5
H_3BO_3	25
Saccharin	3

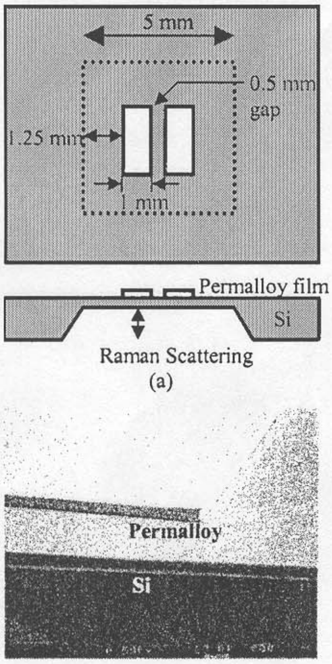

Fig. 2. Fabricated silicon membrane with permalloy film: (a) schematic view (b) cut view.

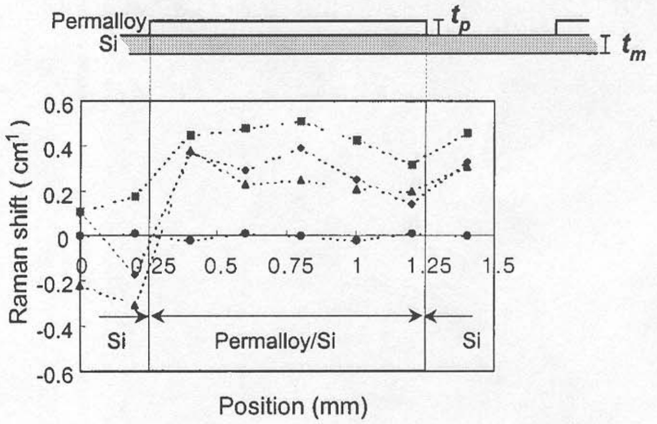

Fig. 3. Raman shift corresponding to stress distribution, which is measured on the silicon membrane, where t_p/t_m is: ■ 6/9 ◆ 13/9.5 ▲ 13/12 • 13/34 (unit of t_p and t_m: μm).

electroplating, the photoresist was stripped with acetone and Cr (300 Å)/Cu (3000 Å) layers on nonelectroplated area were removed. Fig. 2 shows schematic and actual view of the membrane. The Raman scattering facility included an instrument, SA model T64000 equipped with a triple monochromator, a liquid N_2 cooled CCD detector and a microscope attachment. The scattering was excited with 514.1 nm line from Ar^+ laser and the beam was brought to a sharp focus of less than 2 μm. Raman shifts were recorded by systemically moving a sample on the microscopy X–Y stage. The frequency of silicon Raman peak from nonmembrane region was taken as the stress-free reference value, ω_0.

The same testing structure was used for a magnetic microvalve for fast implementation and modification of the design based on the stress analysis. The characterization of magnetic microvalve was performed with external current source and N_2 gas.

III. RESULTS AND DISCUSSION

The profile of the Raman shift representing local stress distribution is shown in Fig. 3. Compressive stress is observed in all the membranes except the membrane with thickness, $t_m = 34$ μm. Though larger stress is found in thinner silicon membranes with the same permalloy films, the membrane thickness (t_m) affects considerably the magnitude of frozen-in stress, which is obvious when we compare 6 μm permalloy/9 μm silicon, 13 μm permalloy/9.5 μm silicon with 13 μm permalloy/12 μm silicon, 13 μm permalloy/9.5 μm silicon.

Several researchers have studied the mechanical stress caused by a thin film on a substrate. It is found in general that the induced stress is small in a substrate, provided the deposited film thickness is much smaller than the substrate thickness [5]. However, the frequently used structure in MEMS devices consists of thin membrane substrate in many cases. Accordingly, the measured results show abrupt changes in local stress near boundaries of films from compressive to tensile. The behavior has also been reported in other reports and explained by an edge force originated at the film edge and acting parallel to the surface, to hold films and the vertical force acting on the edge separating films from the surface [5], [6]. For thin membranes, residual stress acts as a bending force causing the silicon membrane deformation and finally device failure. Furthermore, stress is not fully released near the film edge facing the beginning of another film at positions between 1.25 mm and 1.50 mm in Fig. 3. As a result, an uneven stress distribution over the silicon membrane occurs and causes membrane distortion and even limits mechanical stability of a device.

A stress-free condition is found by plotting Raman phonon shift as a function of silicon membrane thickness (t_m) in Fig. 4. Raman shift is measured at a spot, located at a distance of 0.8 mm from the edge of the film. At a fixed thickness of permalloy film, $t_p = 13$ μm, thickness of silicon membrane, t_m should be around 34 μm to avoid stress appearing on the membrane. Though it is possible to prevent residual stress with thinner permalloy films or with thicker silicon membrane, there is functional compromise between the dimensional controls. If the total volume of permalloy film is reduced, it becomes more difficult to get enough magnetic force to actuate the whole membrane. If the thickness of the silicon membrane is increased, much larger force is required for the membrane to move.

Based on the stress analysis, the flat stress-free silicon membrane with electroplated permalloy film is found to be

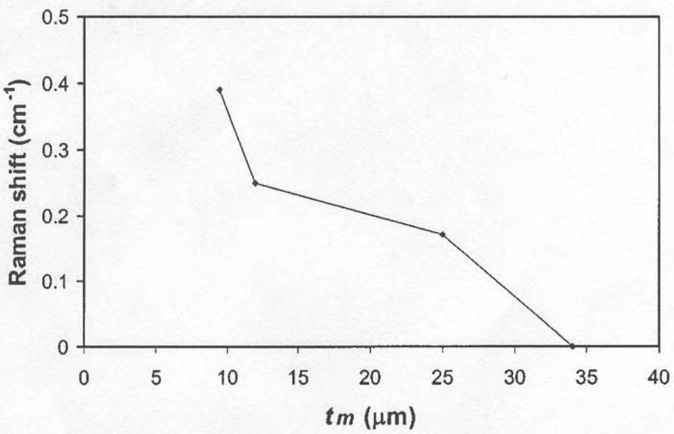

Fig. 4. Raman shift variation as a function of silicon membrane thickness, t_m ($t_p = 13\ \mu$m).

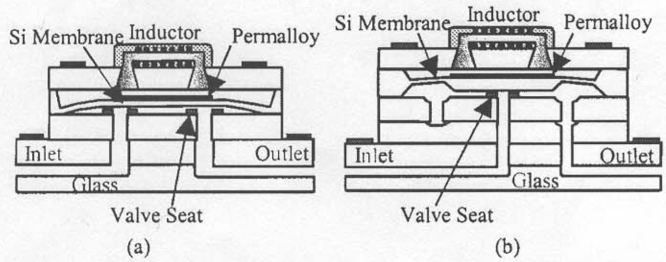

Fig. 5. Schematic view of a microvalve structure using (a) flat membrane and (b) mesa membrane.

a challenging structure for MEMS actuators. To address and solve this mechanical reliability issue, the mesa structure was devised and fabricated as a part of a silicon membrane type microvalve. The permalloy films were electroplated only on the thick portion of the silicon substrate and the movable area was made with thin membrane. In this structure, while the residual stress appearing on the membrane is prevented by the thick mesa structure, the required magnetic force can be kept low by using a thin moving membrane. In Fig. 5, a schematic diagram of design modification is shown.

Flow rate as a function of actuation current is plotted in Fig. 6 for a microvalve, which consists of either a flat membrane or a mesa membrane. Though the mesa structure adds more mass than the flat membrane structure, by designing the mesa membrane, the leakage under low current condition was considerably suppressed.

IV. Conclusion

In this work, we have used the Raman optic phonon shift as a measure of frozen-in stress on silicon membranes electroplated with permalloy films. Based on the stress distribution, new mesa membrane was devised and implemented for improving the fluidic function of a microvalve. Compressive stress is

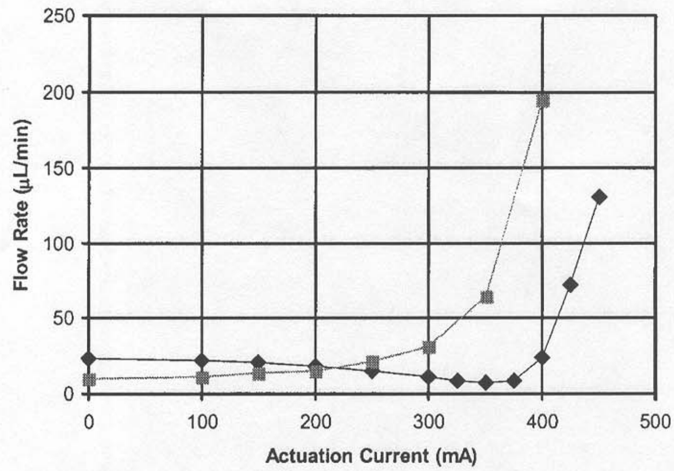

Fig. 6. Flow rate of nitrogen gas as a function of actuation current, ♦ flat membrane ■ mesa membrane.

observed over silicon membranes with electroplated permalloy films. The thickness of the silicon membrane is the principal factor determining the local stress rather than the thickness of the permalloy film. The change of local stress from compressive to tensile is observed at the edges of permalloy films. A mesa membrane was fabricated and integrated successfully in the microvalve to prevent residual stress from the interface with electroplated permalloy films and suppress the low flow leakage. Such a nondestructive and noncontact microscopic stress analysis technique was demonstrated as powerful tool for design optimization in various magnetic MEMS devices.

Acknowledgment

The authors would like to thank Mr. D. Georgiev and Mr. D.-S. Lee of the University of Cincinnati for the technical assistance in measurements.

References

[1] J. W. Judy and R. S. Muller, "Magnetically actuated, addressable microstructures," *IEEE J. Microelectromech. Syst.*, vol. 6, no. 3, pp. 249–255, 1997.
[2] Y. W. Yi and C. Liu, "Magnetic actuation of hinged microstructures," *IEEE J. Microelectromech. Syst., Trans.*, vol. 8, no. 1, pp. 10–17, 1999.
[3] D. S. Sadler *et al.*, "A new magnetically actuated microvalve for liquid and gas control applications," in *Transducers '99: The 10th International Conference on Solid-State Sensors and Actuators*, Sendai, Japan, 1999, pp. 1812–1815.
[4] M. S. Benrakkad *et al.*, "Stress gradient and structural properties of atmospheric and reduced pressure deposited polysilicon layers for micromechanical sensors," *Sensors and Actuators*, vol. A51, pp. 9–12, 1995.
[5] I. D. Wolf *et al.*, "Micro-Raman study of stress distribution in local isolation structures and correlation with transmission electron microscopy," *J. Appl. Phys.*, vol. 71, no. 2, pp. 898–906, 1992.
[6] S. C. Jane *et al.*, "Stresses and strains in lattice-mismatched stripes, quantum wires, quantum dots, and substrates in Si technology," *J. Appl. Phys.*, vol. 79, no. 11, pp. 8145–8165, 1996.